T.3: Fundamental physical properties of InP/GaAs based type-II ultrathin quantum wells

S. D. Singh
Materials Research Lab., Indus Synchrotrons Utilization Division, RRCAT Indore
devsh@rrcat.gov.in

Introduction

Quantum structures like quantum wells (QWs), quantum wires, and quantum dots (QDs) are of current interest because opto-electronic devices utilizing these structures have shown superior device properties as compared to the bulk structures [1, 2]. Quantum structures can have type-I or type-II band alignment. For type-I QW systems, both type of carriers (electrons and holes) are confined in the QW region, which leads to an increased overlap of electron and hole wave functions and hence these structures show high radiative recombination efficiency. Thus, quantum structures based on type-I band alignment systems such as GaAs/AlGaAs, InAs/GaAs, and InAs/InP are commonly used in the development of efficient light emitting devices like light emitting diodes and laser diodes [1]. On the other hand, for type-II systems like InP/GaAs, GaSb/GaAs, and SiGe/Si, only one type of carrier is confined in the well region, while the other carrier is in the barrier region. These structures suffer from the poor overlap of electron and hole wave functions and hence cannot be used in light emitters. This is the reason that the type-II quantum structures are less explored as compared to the type-I systems. However, type-II structures exhibit interesting physical phenomenon of Aharonov Bohm oscillations [3] in their optical spectrum and also have found applications in photodetectors, optical memory devices, and solar cells [4].

Highly strained ultrathin QW presents unique electronic and optical properties [5]. These structures are also very interesting because they represent the limit of decreasing well width for two dimensional (2D) QW structures [6]. Apart from these interesting physical properties, InAs/GaAs ultrathin QWs are used in the diode lasers with high gain excitonic lasing [7]. InP/GaAs material system also has a large strain (~3.8%) and the band alignment between them is believed to be type-II [8]. However, comprehensive study of fundamental physical properties is lacking on this system [8, 9]. This article presents detailed structural, optical and electrical properties of InP/GaAs type-II ultrathin QWs.

Metal organic vapour phase epitaxy (MOVPE) growth of ultrathin QWs

Investigated ultrathin QWs were grown by using MOVPE technique. This technique provides excellent control over interfaces and growth rates, which makes it suitable for the growth of such ultrathin QWs. At first one multiple quantum well (MQW) was grown to estimate the thickness of ultrathin QWs. Thereafter, four ultrathin QWs of varying QW thickness from 2.14 MLs, 1.43 MLs, 0.95MLs, and 0.72MLs were grown at 600^{0}C growth temperature at 50mbar of reactor pressure to investigate the fundamental physical properties. V/III ratios for GaAs barrier layer and InP QW were ~100 and ~250 respectively. The typical growth rates for GaAs and InP layers were 2.5Å/s and 0.4Å/s. The cap and barrier layers of GaAs were doped with Si to provide n-type doping density of 3-4x10^{17} cm^{-3}.

Structural properties of ultrathin QWs

Crystalline and interfacial qualities of grown ultrathin QWs were investigated by using high resolution x-ray diffraction (HRXRD) and transmission electron microscopy (TEM) techniques. Figure T.3.1 shows HRXRD pattern for (004)

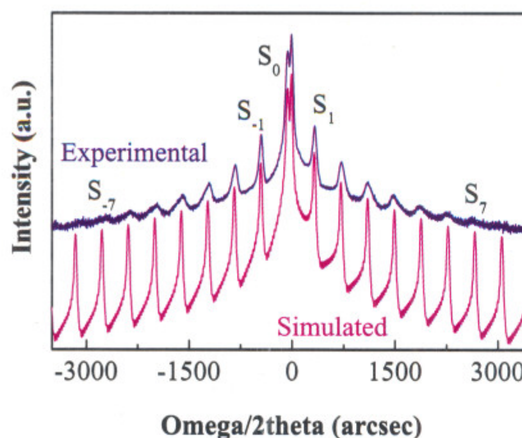

Fig T.3.1 Experimental and simulated HRXRD profiles for (004) symmetric reflection of MQW sample.

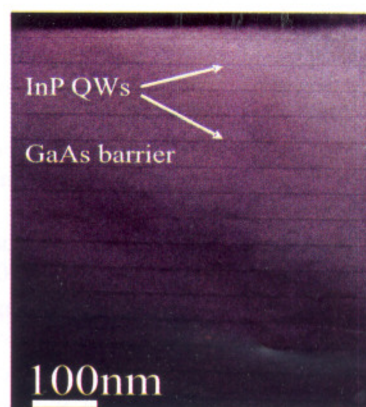

Fig T.3.2 Cross-sectional TEM image of MQW sample.

symmetric reflection from MQW sample, which contains 15 numbers of InP QWs separated by GaAs barrier layers. We clearly observe superlattice peaks up to 7th order, which confirms high interfacial and crystalline qualities. These superlattice peaks originate due to the artificially created periodicity along the growth direction. Thicknesses of InP QW and GaAs barrier layers were estimated by simulating the diffraction profile as shown in the Fig. T.3.1. The thickness values are 0.28±0.01nm (0.95±0.04MLs) and 48.5nm for InP QW and GaAs barrier layer respectively. Figure T.3.2 shows the cross-sectional TEM image for the same MQW sample, where 15 InP QWs are observed as thin black lines separated by GaAs barrier layers. The period thickness (InP QW and GaAs barrier thickness) of ~50nm is measured from this image which corroborates with that is determined from the HRXRD data. HRXRD pattern from all the ultrathin QW samples are shown in Fig. T.3.3, where well defined Pendellosung fringes around the GaAs substrate peak are observed. These fringes arise due to the interference of x-rays diffracted from the GaAs cap layer and the substrate separated by InP ultrathin QW [5].

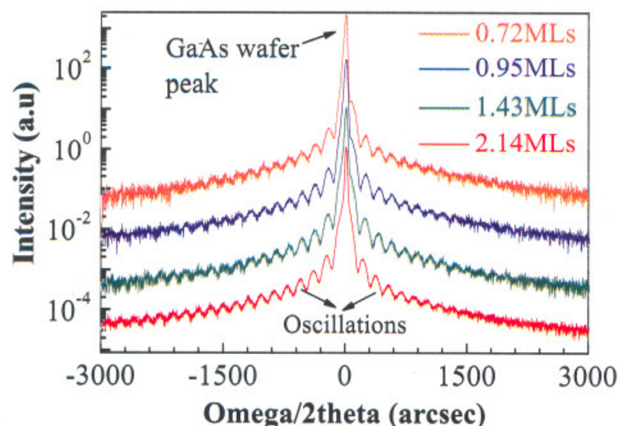

Fig T.3.3 HRXRD profiles for ultrathin QWs.

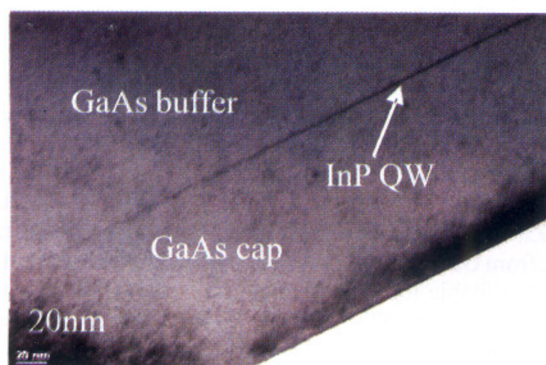

Fig T.3.4 Cross-sectional TEM image for 1.43MLs thick ultrathin QW.

A separate peak corresponding to InP ultrathin QWs is not observed in the HRXRD data because of the very small thickness of the QWs. Therefore, clear observation of Pendellosung fringes around the GaAs substrate peak indicates the high crystalline and interfacial qualities of MOVPE grown ultrathin QW structures.

Figure T.3.4 shows the cross sectional TEM micrograph for one of the ultrathin QW sample (1.43MLs thick QW) as a representative, where InP ultrathin QW is observed by a thin black line at ~120nm from the top surface. Any signature of line defects like dislocations is not observed in the high resolution TEM image (not shown here) which indicates that the large strain (~3.8%) between InP and GaAs is easily accommodated in the ultrathin QWs. Thus, pseudomorphic growth of the ultrathin QWs is demonstrated from these two characterization techniques.

Type-II band alignment at InP/GaAs hetero-inteface

Optical properties and band alignment of these ultrathin QWs were investigated using photoluminescence (PL) technique. Figure T.3.5 shows 10K PL spectra, where intense PL from all the ultrathin QWs is observed in 1.40-1.48eV energy range apart from relatively weak band edge (~1.52eV)

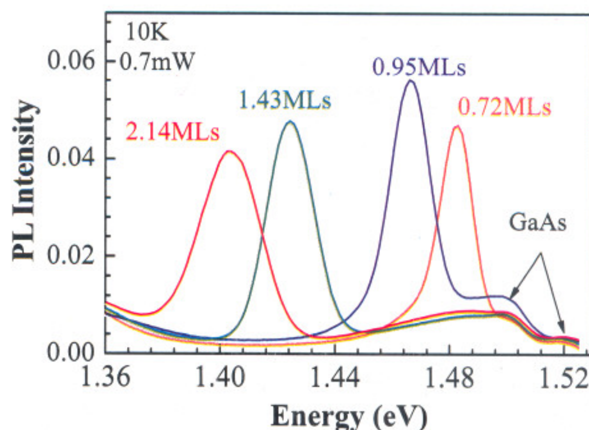

Fig T.3.5 10K PL spectra for ultrathin QWs.

and carbon related (~1.49eV) features from GaAs barrier layer. It is observed that PL peak shifts to higher energy when QW thickness is reduced, which confirms that observed PL is related to QWs. Transition energy obtained from the Gaussian fitting is 1.403eV, 1.424eV, 1.466eV, and 1.482eV for the QW width of 2.14MLs, 1.43MLs, 0.95MLs, and 0.72MLs respectively [10]. It is to be noted that the transition energy of 2.14MLs thick QW is less than the band gap energy of InP material (~1.424eV) itself. This observation suggests that the observed PL is related to the recombination of spatially separated electron and hole pairs in type-II band alignment system as schematically drawn in the inset of Fig. T.3.6(a); because, in a type-I band alignment system, QW transition

energy is always greater than the band gap energy of QW material. It has been reported that if a QW structure has type-II band alignment then transition energy blue shifts with the excitation power (P) and increases linearly with the cube root of excitation power ($P^{1/3}$) [4, 10]. The cube root behaviour is related to the hole which is confined in a triangular potential well formed at the hetero-interface of QW and barrier layer as shown in inset of Fig. T.3.6(a). The steepness of triangular potential well increases with the increase in laser excitation power in PL measurements. This leads to increase in the energy of confined hole leading to the blue shift in the QW transition energy. Detailed theoretical analysis has shown that the energy of hole confined at the triangular potential is proportional to the cube root of the laser excitation power ($P^{1/3}$) [11]. Figure T.3.6(a) shows a graph between transition energy and $P^{1/3}$ for 2.14MLs thick QW. It is observed that the data are nicely fitted with a straight line. Data for other QWs also show similar behaviour, which confirms that the band alignment between InP and GaAs is type-II [10].

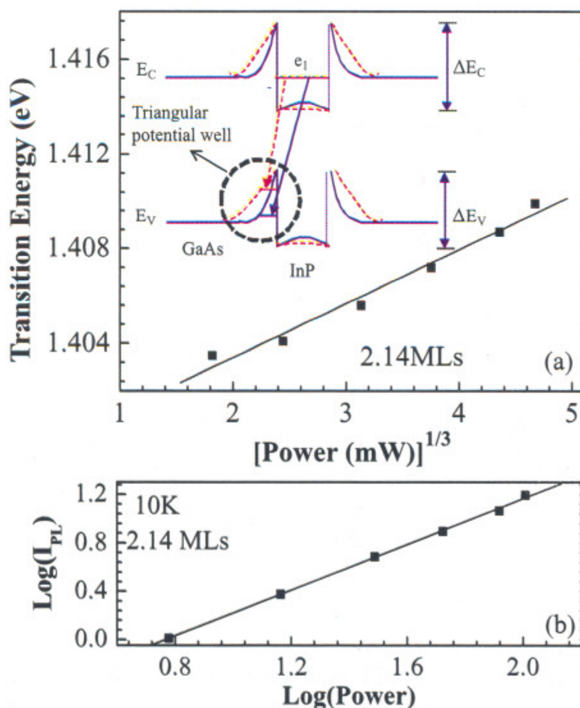

Fig T.3.6 (a) Linear behaviour of QW transition energy on cube root of excitation power. Inset of Fig. (a) shows the QW band diagram at low and high excitation conditions. (b) Linear variation of integrated PL intensity on excitation power.

Further, the recombination process can also be identified from intensity dependent PL measurements. It has been shown that the PL intensity $I_{PL} \alpha I_{ex}^{\beta}$, where I_{ex} is the excitation intensity and $\beta = 1$ for excitonic recombination, $\beta = 2$ for free carrier recombination, and for $1 < \beta < 2$ there is an interplay between free carrier and excitonic recombination [10]. Figure T.3.6(b) shows a log log plot between integrated PL intensity and excitation power along with a linear fit for 2.14MLs thick ultrathin QW at 10 K. The other QW samples also show similar behaviour and the measured value of β is 1.0, 1.1, 1.1, and 1.1 for QWs thickness of 2.14MLs, 1.43MLs, 0.95MLs, and 0.72MLs, respectively. Hence, observed PL at 10K is of excitonic nature for all the ultrathin QWs.

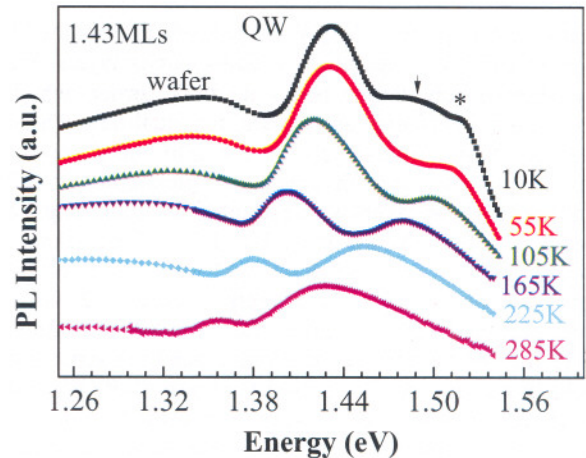

Fig T.3.7 Temperature dependent PL spectra for 1.43MLs thick ultrathin QW.

Temperature dependence of transition energy and luminescence loss mechanism for ultrathin QWs

Temperature dependent PL of bulk semiconductors (quantum structures) is not only used to investigate the electron-phonon interaction but it also provides important information about the luminescence loss mechanism, which is highly desirable from the point of view of optoelectronic device operation [5, 12, 13]. For this, temperature dependent PL measurements in 10-300K temperature range were performed on two ultrathin QWs (1.43MLs and 0.95MLs). This is because PL peak from 0.72MLs QW being nearer to band edge PL of GaAs merges in it with increase in temperature [12]. Similarly, PL peak of 2.14MLs thick QW being nearer to wafer peak merges in it with rise in temperature. However, the PL peaks for 1.43MLs and 0.95MLs thick QWs are relatively farther from the band edge PL from GaAs barrier layer and the wafer peak and that makes them suitable for the investigation in the whole temperature range of 10-300K. Figure T.3.7 depicts temperature dependent PL spectra from 1.43MLs thick ultrathin QW, where QW PL intensity is getting reduced with rise in temperature and measurable PL signal could be obtained up to 285K. On the other hand, PL signal from 0.95MLs thick QW

showed similar behaviour and could be measured up to 165K (graph not shown here) [12]. To understand such temperature dependence behaviour, transition energy was determined as a function of temperature by Gaussian fitting of PL spectra. Temperature dependent transition energy can be analyzed by using Bose-Einstein empirical relation and information about the electron-phonon interaction can be obtained. Temperature dependent transition energy using Bose-Einstein empirical relation can be written as [14]

$$E(T) = E_B - a_B\left[1 + \frac{2}{\{\exp(\theta_B / k_B T) - 1\}}\right]$$

where, E_B-a_B corresponds to the transition energy at 0K, a_B is the strength of electron-phonon interaction, and θ_B corresponds to the mean phonon temperature. The temperature dependent transition energy was fitted to Bose-Einstein relation and the obtained values of E_B, a_B, and θ_B for 1.43MLs (0.95MLs) thick QW are 1.497eV (1.528eV), 65meV (59meV), and 277K (232K) respectively. The values of a_B, and θ_B for InP (GaAs) bulk materials are 54meV (60meV), and 274K (252K) respectively. It is to be noted that there is not much difference in the values of a_B, and θ_B for InP

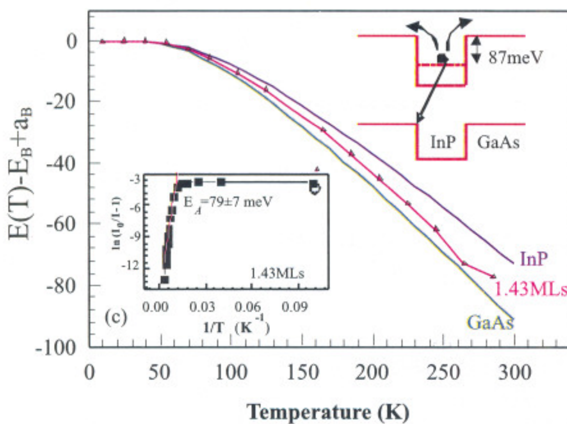

Fig T.3.8 Variation of [E(T)-E_B+a_B] with temperature for 1.43 and 0.95MLs thick QWs. Left inset shows the Arrhenius like plot to determine activation energy. Right inset shows the QW band diagram indicating loss of electrons from QW to barrier region.

and GaAs materials. Hence, on the basis of measured values of a_B and θ_B for ultrathin QWs, we cannot unambiguously determine whether the temperature dependence of the QW transition energy follows the band gap variation of GaAs and/or InP materials. For unambiguous assignment, the values of $E(T) - E_B + a_B$ for ultrathin QWs, GaAs, and InP materials are plotted as a function of temperature in Fig. T.3.8. We clearly note that the temperature dependence of the QW transition energy is similar to that of the GaAs material. This result is consistent with our earlier observation that was made in case of InAs/GaAs ultrathin QW, where temperature dependence of the QW transition energy was found to follow the band gap variation of GaAs barrier material rather than the QW material [5].

The mechanism responsible for the PL quenching at high temperature can be determined by knowing the integrated PL intensity as a function of temperature [12]. The variation of PL intensity (I) with temperature (T) can be described by a phenomenological expression of the following form

$$I = \frac{I_0}{1 + C * \exp(-E_A / k_B T)}$$

where, I_0 is the PL intensity at very low temperature (~0K), C is a constant, and E_A is the activation energy responsible for the quenching of PL intensity with temperature. Thus, if the value of ln(I_0/I-1) is plotted with reciprocal of temperature, then the slope of linear fit give the value of activation energy. Such plot for 1.43MLs thick QW is shown in the left inset of Fig. T.3.8, where experimental data in the high temperature region is nicely fitted with a linear line. The value of activation energy determined for 1.43MLs and 0.95MLs thick QWs is 79±7meV and 44±4meV respectively. It is to be noted that this activation energy corresponds to the energy difference between transition energy and the band gap of GaAs barrier layer as schematically shown in the right inset of Fig. T.3.8. Thus, thermal emission of electrons from the QWs to the GaAs barrier layer is found to be the prime cause for the quenching of PL intensity with temperature [12]. This fact is also supported by the observation that the PL intensity of GaAs barrier layer increase with temperature as observed from Fig. T.3.7.

Observation of room temperature optical absorption in ultrathin QWs

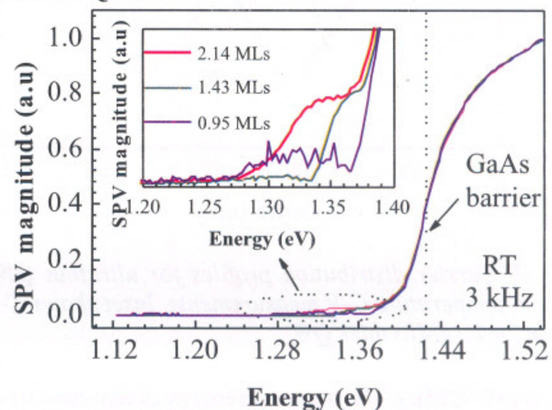

Fig T.3.9 Room temperature SPS spectra from ultrathin QWs. Inset shows the enlarged view to clearly observe the absorption edge of ultrathin QWs.

It has been observed that PL from one ultrathin QW (1.43MLs) could be measured at near room temperature (285K). However, it is desirable to know the transition energy of ultrathin QWs at room temperature from the optoelectronic device operation point of view. It is also noted from the luminescence loss mechanism that the carriers are suffered from the thermal loss to the GaAs barrier layer. This means that the carriers are getting separated or recombining in the barrier region after generation. Hence, the information about the transition energy at room temperature can be obtained through some technique that depends on the separation of carriers. Surface photovoltage spectroscopy (SPS) is one of the techniques based on carrier separation. In SPS technique, change in surface potential due to the separation of charge carriers subsequent to photo generation is measured and the information about transition energy is obtained as described in literature [15]. Figure T.3.9 shows SPS spectra at room temperature for three ultrathin QWs (2.14, 1.43, and 0.95MLs thick QWs). The inset to this figure presents the enlarged view of the same spectra to clearly observe the absorption edges related to ultrathin QWs. Significant absorption below the band gap energy (~1.424eV) of GaAs barrier layer is noted in SPS spectra of ultrathin QWs. The absorption edge of ultrathin QW shifts to higher energy with decrease in QW thickness from 2.14MLs to 1.43MLs and finally it merges with that of GaAs barrier layer with further decrease in QW

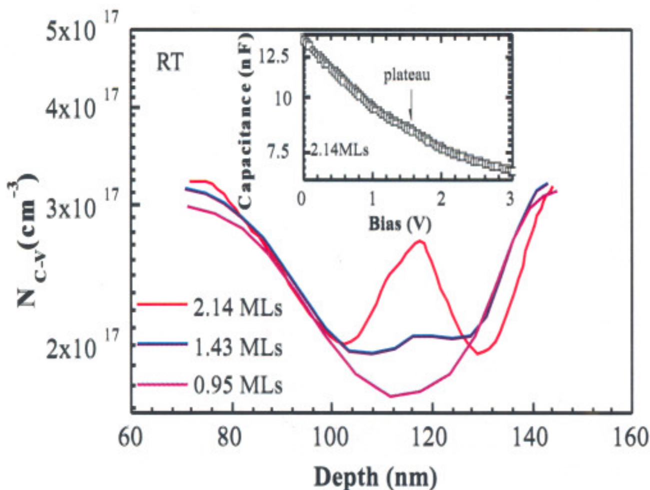

Fig T.3.10 Carrier distribution profiles for ultrathin QWs from room temperature C-V measurements. Inset shows C-V spectrum for 2.14MLs thick QW.

thickness to 0.95MLs. The transition energy determined from the room temperature SPS spectra is ~1.32eV and ~1.35eV for QW thickness of 2.14MLs and 1.43MLs respectively. Hence, these results suggest that SPS technique is capable of detecting absorption in QWs having ultrathin thicknesses (~1 MLs) at room temperature.

Electron confinement in the conduction band of InP ultrathin QWs

Carrier distribution characteristics play a very important role in determining the optimum performance of optoelectronic devices [16].

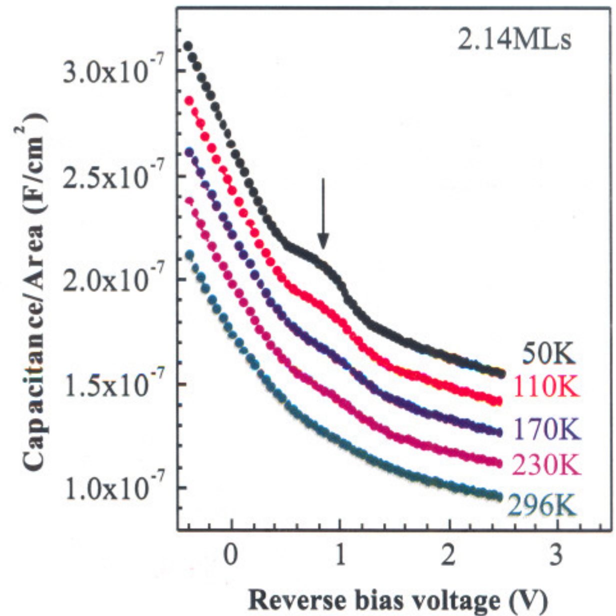

Fig T.3.11 Temperature dependent C-V characteristics for 2.14MLs thick ultrathin QW.

Capacitance–voltage (C–V) measurements have been used to obtain the carrier distribution profiles in bulk as well as quantum structures like QDs and QWs [16]. In C-V measurements, one measures capacitance at different reverse bias and then carrier distribution profiles are obtained by using the following relation

$$N(w) = -\frac{2}{e\varepsilon\varepsilon_0 A^2 \dfrac{\partial(C^{-2})}{\partial V}} \qquad w = \varepsilon\varepsilon_0 A / C$$

where, ε_0 and ε are the permittivity of free space and dielectric constant of semiconductor. $N(w)$ is the carrier concentration at depth (w) from the top surface. Capacitance is measured by making Schottky contact at the cap layer (top side) and Ohmic contact at the buffer layer or substrate (bottom side) of the QW sample. The cap layer is depleted up to a certain depth, known as depletion width, from the free carriers, when

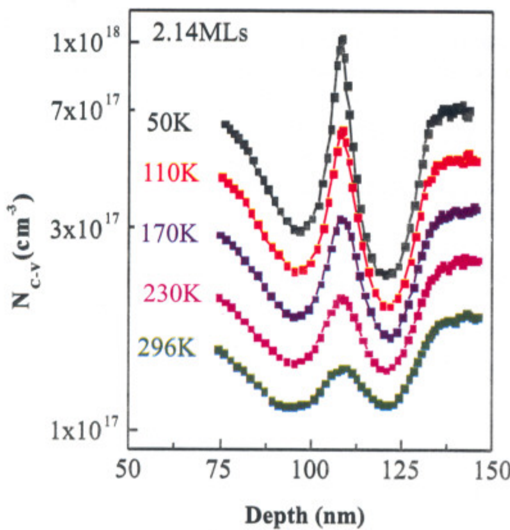

Fig T.3.12 Carrier distribution profiles at different temperatures for 2.14MLs thick ultrathin QW.

Schottky contact is made on it. This structure has a finite capacitance at zero bias, which decreases with increase in reverse bias voltage due to increase in the depletion width of the cap layer having a constant doping density. As the depletion width approaches the QW region with the increase in reverse bias voltage, capacitance varies very slowly because of a large number of carriers present in the QW, which screen the applied electric field. These carriers are 2D carriers occupying the quantum states formed in the QW region. When the applied reverse bias voltage is large enough to sweep out all the carriers present in the QW, capacitance again decreases following an increase in the depletion width of the buffer layer having constant doping density. Thus, a plateau region is observed in the C–V profile for a QW structure. Inset to Fig.T.3.10 shows C-V characteristic for 2.14MLs thick QW, where a weak plateau region is observed between 1-2V of reverse bias region. A well defined peak in the carrier distribution profile is observed at around the geometrical position of the ultrathin QW as shown in Fig. T.3.10. It is noted that this peak gets diminished for a QW thickness of 1.43MLs and finally it disappears for the QW thickness of 0.95MLs. This observation suggests that the accumulated peak at around the QW region is related to the electrons confined in InP QW. This is also confirmed from the detailed analysis of temperature dependent C-V measurements, which are shown in Fig. T.3.11. It is noted that the observed plateau is gradually becoming stronger with the reduction in temperature, which is very well defined at 50K.

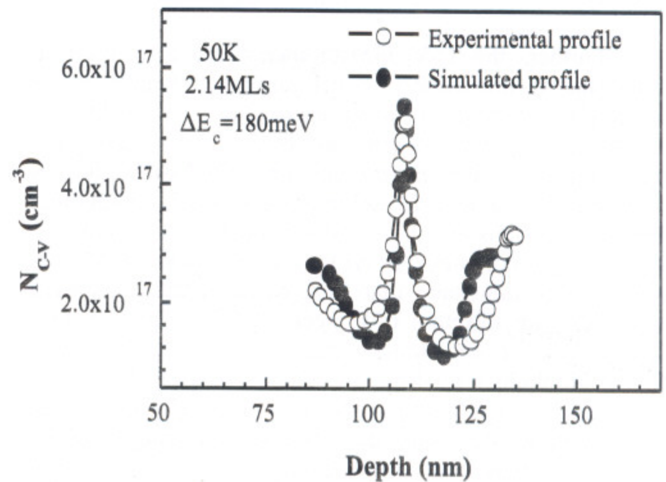

Fig T.3.13 Simulated as well as experimental carrier distribution profiles for 2.14MLs thick QW.

This observation suggests that the density of carriers increases with the decrease in temperature. It also becomes clear when the carrier distribution profiles at different temperatures are plotted in Fig. T.3.12. We note that the carrier density accumulated at around the geometrical position of the QW increases with decrease in temperature. This is due to increase in the separation between Fermi level and quantum state (confined electronic level in the QW) as well as decreased probability for thermal emission of electrons into the barrier region as a result of decreased thermal energy with the reduction in temperature. Another important observation made from Fig. T.3.12 is that the width of carrier distribution profiles is getting reduced with decrease in temperature. This has been understood in terms of relative contribution of three dimensional (3D) carriers of barrier region and 2D carriers of the QW at different temperatures. It is shown from the theoretical calculations that the width of carrier distribution profiles at low temperatures is given by the position expectation value of 2D carriers because of the negligible contribution from 3D carriers [17]. However, at higher temperatures, the contribution of 3D carriers cannot be neglected and the width is governed by Debye averaging process between 2D and 3D carriers, which increases with rise in temperature. Increase in the carrier density and decrease in the width of the carrier distribution profiles with reduction in temperature have been attributed to the finger prints of the 2D carriers occupying the quantum states formed in the QWs. Hence, it is confirmed that the observed peak in carrier distribution profiles at around the geometrical position of the ultrathin QWs is due to 2D electrons confined in the conduction band of InP QWs.

Further, the C-V measurements are also used to determine an important physical parameter, known as the band offset, at the hetero-junctions or QWs. This is done by simulating the carrier distribution profiles by adjusting the band offset at the hetero-junction. The simulation is performed by numerically solving coupled Schrodinger and Poisson equations in a self-consistent manner under envelop function approximation (EFA) for a QW structure [18]. It is important to note here that EFA based calculations have limitations for ultrathin QW, because EFA approximation breaks down for such ultrathin thicknesses [5, 16]. However, for the simplicity it has been used to explain the experimental observations of ultrathin QW and produced results are comparable to the results that are obtained using involved calculations based on tight binding and pseudopotential. Figure T.3.13 shows experimental as well as simulated carrier distribution profiles for 2.14MLs thick ultrathin QW. A reasonable agreement between experimental and simulated profiles is noted for the conduction band offset value of 180meV, which is consistent with that determined from photoelectron spectroscopy measurements [16].

Conclusion

Ultrathin InP/GaAs QWs with excellent crystalline and interfacial qualities are grown by MOVPE technique as confirmed from TEM, HRXRD, and PL measurements. Intense excitonic PL from these ultrathin QWs is observed at low temperatures. Type-II band alignment of InP/GaAs ultrathin QWs have been confirmed from the cube root dependence of transition energy on laser excitation power. Near room temperature PL from one of the ultrathin QW is observed at room temperature. Thermal loss of the electrons to the GaAs barrier layer is found to be the main cause of the quenching of PL intensity with temperature. SPS technique has been found to be useful in determining the transition energy of the ultrathin QWs at room temperature, where no PL signal could be detected from the ultrathin QWs. Conduction band offset at InP/GaAs hetero-junction has been obtained by simulating the C-V profile of the ultrathin QW.

Acknowledgements

This work has been carried out in Semiconductor Laser Section, Solid State Laser Division as a part of the Ph. D. thesis. Author acknowledges his thesis advisors Dr. A. Chakrabarti and Dr. T. K. Sharma for their invaluable guidance and discussions/suggestions throughout this work. The author also acknowledges his Ph. D. committee members Dr. S. M. Oak, Dr. S. K. Deb, and Dr. L. M. Kukreja for their critical suggestions, guidance, and motivation during the course of this work. Dr. Tapas Ganguli, Dr. V. K. Dixit, Dr. A. K. Srivastava, Dr. C. Mukherjee, and Dr. S. Pal are gratefully acknowledged for their guidance, support in experiments, and motivation throughout the work. It is the support from Shri S. K. Khamari, Shri R. Kumar, Shri S. Porwal, Shri Mahendra Babu, Shri U. K. Ghosh and Shri Alexander Khakha, which helped me to grow and characterize the QW samples. The author wishes to express his gratitude to Director, RRCAT, Dr. S. K. Deb and Dr. S. M. Oak for giving him the opportunity and necessary support to write this article.

References

1. Chand N., Becker E. E., Ziel J. P. van der, Chu S. N. G., Dutta N. K.
Excellent uniformity and very low (<50 A/cm^2) threshold current density strained InGaAs quantum well diode lasers on GaAs substrate
Appl. Phys. Lett. 58, 1704, (1991).

2. Raghavan S., Forman D., Hill P., Weisse-Bernstein N. R., G. von Winckel, Rotella P., Krishna S., Kennerly S. W., Little J. W.
Normal-incidence InAs/$In_{0.15}Ga_{0.85}As$ quantum dots-in-a-well detector operating in the long-wave infrared atmospheric window (8–12 μm)
J. Appl. Phys. 96, 1036 (2004).

3. Ribeiro E., Govorov A. O., Jr. W. C., Medeiros-Ribeiro G.
Aharonov-Bohm Signature for Neutral Polarized Excitons in Type-II Quantum Dot Ensembles
Phys. Rev. Lett. 92, 126402 (2001).

4. Alonso-Alvarez D., Alen B., Garcia J. M., Ripalda J. M.
Optical investigation of type II GaSb/GaAs self-assembled quantum dots
Appl. Phys. Lett. 91, 263103 (2007).

5. Singh S. D., Porwal S., Sharma T. K., Rustagi K. C.
Temperature dependence of the lowest excitonic transition for an InAs ultrathin quantum well
J. Appl. Phys. 99, 063517 (2006).

6. Tran C. A., Ares R. A., Karasyuk V. A., Watkins S. P., Letourneau G., Leonelli R.
Origin of sharp lines in photoluminescence emission from submonolayers of InAs in GaAs
Phys. Rev. B 55, 4633 (1997).

7. Goni A. R., Stroh M., Thomsen C., Heinrichsdorff F., Türck V., Bimberg D.
High-gain excitonic lasing from a single InAs monolayer in bulk GaAs
Appl. Phys. Lett. 72, 1433 (1998).

8. Wang B., Chua S.-J.
Growth and optical properties of type-II InP/GaAs self-organized quantum dots
Appl. Phys. Lett. 78, 628 (2001).

9. Godoy M. P. F. de, Nakaema M. K. K., Iikawa F., Brasil M. J. S. P., Lopes J. M., Bortoleto J. R. R., Cotta M. A., Magalhães-Paniago R., Mörschbächer M. J., Fichtner P. F. P.
Structural and optical properties of InP quantum dots grown on GaAs(001)
J. Appl. Phys. 101, 073508 (2007).

10. Singh S. D., Dixit V. K., Porwal S., Kumar R., Srivastava A. K., Ganguli T., Sharma T. K., Oak S. M.
Observation of electron confinement in InP/GaAs type-II ultrathin quantum wells
Appl. Phys. Lett. 97, 111912 (2010).

11. Lin C. M., Chen Y. F.
Properties of photoluminescence in type-II ZnMnSe/ZnSeTe multiple quantum wells
Appl. Phys. Lett. 85, 2544 (2004).

12. Singh S. D., Porwal S., Alexander K., Dixit V. K., Srivastava A. K., Oak S. M.
Temperature dependence of the photoluminescence from InP/GaAs type-II ultrathin quantum wells
J. Phys. D: Appl. Phys. 43, 455410 (2010).

13. Allen P. B., Cardona M.
Theory of the temperature dependence of the direct gap of germanium
Phys. Rev. B 23, 1495 (1981).

14. Lautenschlager P., Garriga M., Cardona M.
Temperature dependence of the interband critical-point parameters of InP
Phys. Rev. B 36, 4813 (1987).

15. Sharma T. K., Singh S. D., Porwal S., Nath A. K.
Spectroscopic investigations of MOVPE-grown InGaAs/GaAs quantum wells with low and high built-in strain
Journal of Crystal Growth 298, 527 (2007).

16. Singh S. D., Dixit V. K., Khamari S. K., Kumar R., Srivastava A. K., Ganguli T., Oak S. M.
Conduction band offset and quantum states probed by capacitance–voltage measurements for InP/GaAs type-II ultrathin quantum wells
J. Appl. Phys. 109, 073702 (2011).

17. Moon C. R., Choe B. D., Kwon S. D., Lim H.
Spatial resolution of capacitance-voltage profiles in quantum well structures
Appl. Phys. Lett. 72, 1196 (1998).

18. Dixit V. K., Singh S. D., Porwal S., Kumar R., Ganguli T., Srivastava A. K., Oak S. M.
Determination of band offsets in strained $InAs_xP_{1-x}$/InP quantum well by capacitance voltage profile and photoluminescence spectroscopy
J. Appl. Phys. 109, 083702 (2011).